encit 2022

ABCM Associação Brasileira de Engenharia e Ciências Mecânicas

19th Brazilian Congress of Thermal Sciences and Engineering
November 6th–10th, 2022, Bento Gonçalves - RS - Brazil

ENC-2022-0112
EFFECT OF THIXOTROPY IN COMPLEX FLOWS

Carlos E. Sanchez Perez
Danmer Maza
Marcio S. Carvalho
Department of Mechanical Engineering, Pontifícia Universidade Católica do Rio de Janeiro
Rua Marquês de São Vicente, 225, 22451-900. Rio de Janeiro, Brazil
csanchez@lmmp.mec.puc-rio.br; danmer@lmmp.mec.puc-rio.br; msc@puc-rio.br

Abstract. *Several liquids, in important applications in industry and everyday life, present non-linear behavior and time dependency. These behaviors are associated with microscopic structures that are formed and destroyed during flow. Despite recent developments on time-dependent models, which are able to describe the mechanical behavior of thixotropic fluids, most steady-state complex flow analyses do not take these effects into account. Flow simulations of inelastic, shear-thinning liquids are generally developed by using generalized Newtonian models (GNM). In this case, the viscosity of the liquid is solely a function of the local shear rate, i.e., using the liquid steady-state flow curve. From a material point of view, the deformation rate changes as liquid particles pass through the flow field. Assuming that the viscosity at each point is the steady-state viscosity may lead to inaccurate results. Especially, if the characteristic time of the build-up or the time associated with the destruction of the material structure is in the same order of magnitude of the residence flow time. In this work, we study the flow of a thixotropic liquid through a constricted capillary and near the downstream meniscus of slot coating process. The rheological behavior is governed by a thixotropic model where the typical structure parameter, used in thixotropic modeling, is replaced by fluidity (i.e., reciprocal of viscosity). In this rheological model, the mechanical response is described by two evolution equations: one for the stress and the other for the fluidity. The set of differential equations is solved by the Finite Element Method. The results show how the rheological parameters affect the flow behavior for both cases: thixotropic and GNM simulations. Moreover, the results reveal at which conditions time-dependency can be neglected.*

Keywords: *Thixotropy, Generalized Newtonian Fluid, avalanche and construction times, capillary, slot coating*

1. INTRODUCTION

Interesting and important fluids in industry and other human activities differ from the "ideal" Newtonian behavior. The mechanical behavior of structured fluids, such as polymeric solutions, waxy oils, muds, pharmaceutical & cosmetic products, paints, clay suspensions, processed food, among others (Mewis and Wagner, 2009; de Souza Mendes, 2009) cannot be described by a simple linear relationship between stress and rate of strain. Furthermore, despite much of the literature about coating flows focuses on Newtonian fluids, most liquids in coating applications are strongly non-Newtonian (Glass and Prud'homme, 1997). The macroscopic rheological properties of many of them rely on their microscopic structure (Pritchard *et al.*, 2016). As a result, their rheology also has time dependency. For example, particle suspensions which are used in coating applications. However, time dependent behavior tends to be neglected and steady-state values are used instead.

Time-dependent fluids are subdivided into thixotropic, anti-thixotropic (or so-called rheopectic in some literature), and irreversible. Regarding to the thixotropic phenomenon, it is characterized by a gradual breakdown of the fluid internal microstructures under shear. On the other hand, these microstructures eventually build up when the flow is ceased. As a result, thixotropy is a reversible process, but the microstructure change takes time (Barnes, 1997).

Most thixotropic models have a semi-empirical nature ((Mewis and Wagner, 2009)). They are based on two equations: the stress (σ) as a function of the shear rate $\dot{\gamma}(t)$ and the yield stress σ_y, as shown in Eq. (1), and a kinetic-like equation as described in Eq. (2). The latter shows the evolution of a structure parameter (λ), where $\lambda = 1$ represents the maximum micro-structuring level while $\lambda = 0$ represents the minimum.

$$\sigma(t) = \sigma_y[\lambda(t)] + \eta_\lambda[\lambda(t), \dot{\gamma}(t)]\dot{\gamma}(t) + \eta_{\lambda=0}[\dot{\gamma}(t)]\dot{\gamma}(t) \tag{1}$$

$$\frac{d\lambda}{dt} = -k_1\dot{\gamma}^a\lambda^b + k_2\dot{\gamma}^c(1-\lambda)^d \tag{2}$$

The first term on the right-hand side of Eq. (1) is the yield stress, while η_λ and $\eta_{\lambda=0}$ are the structural and residual viscosities respectively. k_1, k_2, a, b, c and d are constants of the kinetic evolution equation.

de Souza Mendes (2009), de Souza Mendes and Thompson (2012, 2013), and de Souza Mendes *et al.* (2018) have used mechanical analogues, as shown in Fig. 1, with the intention to unify thixotropic models. In addition, de Souza Mendes *et al.* (2018) replaced the structure parameter (λ) for a more meaningful parameter: fluidity. Actually, the latter is the reciprocal of viscosity. Furthermore, this rheological model is based on parameters obtained experimentally. Previous works, like that by Fredrickson (1970), also proposed the use of fluidity instead of the structure parameter.

Besides the thixotropic characterization, measurement and modeling; there are many challenges in incorporating these models into actual flow simulations. In the case of mixers, Barnes (1997) argues that the simulations are relatively easy to be done. Actually, the mixer is treated as a viscometer running at the same shear rate as the average shear rate in the mixer. On the other hand, the same author says that the simulation of flows in pipes is very complicated, especially in short ones where a steady-state condition is not reached. He also argues that the analysis is complex and extensive numerical methods are required. For instance, Moisés *et al.* (2018) used the finite volume method to simulate start-up thixotropic flow in a horizontal pipe. Although Sochi (2010) and others give some hints and identify issues to simulate thixotropic flows into porous media or other small-scale examples, the research related is much more limited. As a result, this is one of the main motivations of this work.

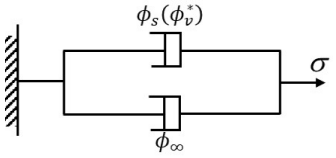

Figure 1. Mechanical analogue of inelastic thixotropic fluids. Adapted from (de Souza Mendes *et al.*, 2018)

The mechanical analogue shown in Fig. 1 is just suitable for inelastic thixotropic fluids, like Laponite suspensions (Siqueira *et al.*, 2020; de Souza Mendes *et al.*, 2018), actually is a simplified version of the analogue used in the work by de Souza Mendes *et al.* (2018). The parameter ϕ_S is the structural fluidity of the liquid which depends on the microstructure level of the liquid. In fact, there is one to one correspondence between the microstructure level and ϕ_v^*. The latter variable is the liquid's normalized fluidity, which varies from 0 to 1. Then, this parameter is related to ϕ_0 and ϕ_∞ (As shown in Eq. (3)); which are respectively the fluidities at maximum and minimum structuring level respectively.

$$\phi_v^* = \frac{\phi_v - \phi_0}{\phi_\infty - \phi_0} \tag{3}$$

$$\text{Where, } 1/\phi_v = 1/\phi_S + 1/\phi_\infty \tag{4}$$

ϕ_v is the actual liquid's fluidity (i.e. reciprocal of viscosity) and it ranges from ϕ_0 to ϕ_∞. In other words, ϕ_0 represents the maximum viscosity of the liquid while ϕ_∞ the minimum one. Furthermore, ϕ_0 is associated with the maximum structuring level of the material while ϕ_∞ is associated with minimum one. ϕ_v considers both structural fluidity and infinity fluidity of the liquid (as shown in Eq. (4)), which are in parallel in Fig. 1. In addition, it is possible to relate the stress ($\boldsymbol{\sigma}$) applied on the liquid to the shear rate ($\dot{\boldsymbol{\gamma}}$) (as shown in Eq. (5)) according to the mechanical analogue presented before.

$$\dot{\boldsymbol{\gamma}} = \phi_v\boldsymbol{\sigma} \tag{5}$$

Siqueira *et al.* (2020) argues that the constituve equation for inelastic thixotropic liquids reduces to that for generalized Newtonian fluids (Eq. (5)) due to the absence of elasticity. However, ϕ_v not only depends on the shear rate (as generalized Newtonian fluids do), it also depends on the shear history. In other words, fluidity also depends on time from a Eularian and Lagrangian frame of reference. Therefore, there would be an evolution equation of fluidity for a particular thixotropic liquid. Actually, de Souza Mendes *et al.* (2018) presented a general evolution equation in their work as shown as follows.

$$\frac{D\phi_v^*}{Dt} = \frac{\partial\phi_v^*}{\partial t} + \mathbf{v}\cdot\boldsymbol{\nabla}\phi_v^* = f\big[\phi_{eq}^*(\sigma), \phi_v^*\big] \tag{6}$$

From Eq. (6) the $\frac{D\phi_v^*}{Dt}$ term is the substantial derivative. Regarding the function $f\big[\phi_{eq}^*(\sigma), \phi_v^*\big]$ is obtained from experimental data from rheological tests, which are performed for a particular liquid. In addition, $\phi_{eq}^*(\sigma)$ corresponds to a

normalized fluidity obtained after achieving an equilibrium condition. Therefore, it is necessary to wait enough time to get this condition (i.e., the measuring of viscosity should be done after some time). Then, $\phi^*_{eq}(\sigma)$ is related to the liquid's flow curve. Besides the time dependency and hysteresis phenomena of thixotropic fluids, there is an unique flow curve for a particular liquid from this category.

In the present work, it was studied thixotropic flows in a steady state condition. As a result, $\frac{\partial \phi^*_v}{\partial t} = 0$. On the other hand, the convective term ($\mathbf{v} \cdot \boldsymbol{\nabla} \phi^*_v$) from the evolution equation is kept, obtaining Eq. (7). As a result, the time dependency was studied from a Lagrangian frame of reference. Then, the convective term is related to the fluid's residence time (t_{Res}) into the domain. Regarding the function $f\big[\phi^*_{eq}(\sigma), \phi^*_v\big]$ is related to the fluid's characteristic times, such as avalance and construction times (t_a and t_c respectively). The physical meaning of t_a is associated with the time required for a thixotropic material to start flowing. On the other hand, t_c is related to the time required to the fluid's microstructure reconstruction after the liquid stopped flowing.

$$\mathbf{v} \cdot \boldsymbol{\nabla} \phi^*_v = f\big[\phi^*_{eq}(\sigma), \phi^*_v\big] \tag{7}$$

To avoid confusion, the generalized Newtonian model (GNM) expression is only used, in the present work, to talk about a rheological model where fluidity (or viscosity) is estimated just considering the fluid's local shear rate (For a given temperature and pressure). On the other hand, thixotropic fluids are referred to fluids whose viscosity depends on the local shear rate as well as the fluid's characteristic times (i.e., t_a and t_c), and residence time (t_{Res}).

There are two flow applications of thixotropic liquids in the present work, both are related to flows at smale scale. Firstly, it was studied thixotropic flows into a constricted capillary (shown in Fig. 3) . In the case of Newtonian flows through a porous media, the bulk flow is easily described by using a constant viscosity. On the other hand, Eberhard *et al.* (2019) implies the necessity of an accurate estimation of the local viscosity for non-Newtonian fluids to have reliable results. The second flow application is a coating application. Actually, coating is an industrial process where one or more liquid layers are deposited on a surface; then they are dried or cured to form solid films to serve for a particular purpose (Kisler and Schweizer, 1997) . Specifically talking, the other flow application presented here is slot coating. In fact, this technique is used in the manufacturing of many products. This method is classified into the category of *premetered methods*, where the thickness of the coated liquid layer only depends on the flow rate of the liquid fed into the coating die (Carvalho and Kheshgi, 2000). As a result, slot coating is one of the preferred coating methods due to its precision (Carvalho and Kheshgi, 2000). An sketch of a typical slot coating device is presented in Fig. 2. However, we focused our study near the downstream meniscus of slot coating process in the present work.

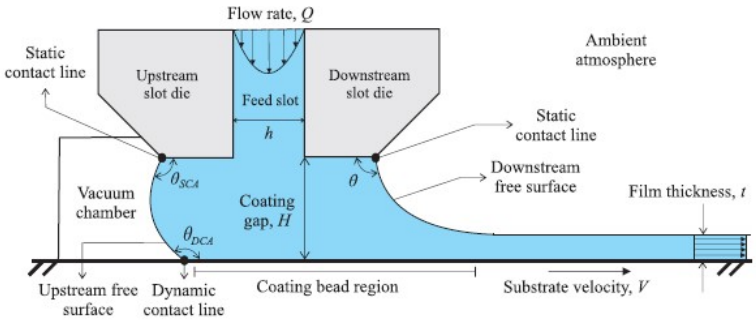

Figure 2. Details of a typical slot coating device (Rebouças *et al.*, 2018)

2. MATHEMATICAL MODEL AND METHODOLOGY

2.1 Thixotropic flow through a constricted capillary

The thixotropic liquid used in the simulations corresponds to a Laponite suspension, which is an inelastic liquid as mentioned by Siqueira *et al.* (2020); de Souza Mendes *et al.* (2018). A sketch of the constricted capillary, including the appropriate boundary conditions, is shown in Fig. 3. The suspension can be treated as a continuum, and the governing equations: mass and momentum conservation equations can be found as Eqs. (8) & (9) :

$$\nabla \cdot \mathbf{v} = 0 \tag{8}$$

$$\rho(\mathbf{v} \cdot \nabla \mathbf{v}) - \nabla \cdot \mathbf{T} = 0 \tag{9}$$

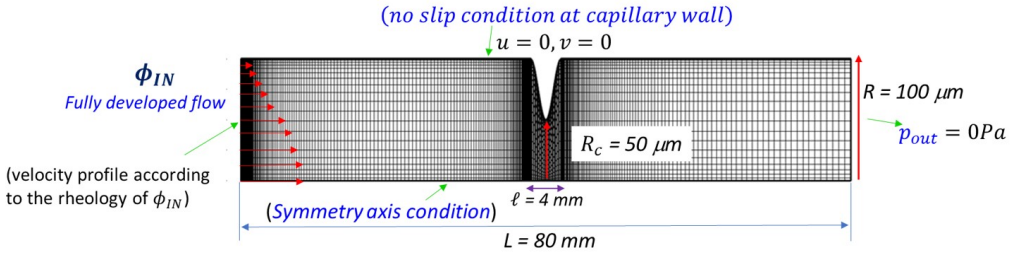

Figure 3. Sketch of the constricted capillary used in the simulations

$$\text{Where, } \mathbf{T} = -p\mathbf{I} + \eta_v \boldsymbol{\sigma} \tag{10}$$

The Eularian velocity vector is given by $\mathbf{v}$. The Cauchy tensor ($\mathbf{T}$) is expressed by Eq. (10). $\boldsymbol{\sigma}$ and $\mathbf{I}$ represent the extra-stress, and the identity tensors respectively. p is the mechanical pressure (Rebouças *et al.*, 2018) while η_v is the suspension's viscosity. The domain was discretized in a refine mesh as shown in Fig. 3. Then Eqs. (8) & (9) were solved by using the Finite Element Method. Specifically, the Galerkin method was used; including quadrilateral elements. If we have a GNM fluid, it is just necessary to have an expression which relates η_v to the shear rate or stress. In the case of a thixotropic fluid, this is possible just at equilibrium. It means that the thixotropic microstructure needs enough time to accomodate itself to the conditions imposed and achieve an equilibrium between the breaking and building up forces. As a result, the substancial derivative ($\frac{D\phi_v^*}{Dt}$) in Eq. (6) is equal to zero. de Souza Mendes *et al.* (2018) proposed an expression of normalized fluidity (ϕ_{eq}^*) at equilibrium for the Laponite suspension used in their work. As fluidity is the reciprocal of viscosity, the Eq. (11) can be used to estimate η_v and solve the governing equations Eqs. (8) & (9) . Actually, the solutions obtained by following this procedure were used as GNM solutions. Then, the solutions obtained were compared with those for the thixotropic cases.

$$\phi_{eq}^* = \frac{\frac{1}{\sigma}\left[\frac{|\sigma-\sigma_y|}{K}\right]^{1/n} H(\sigma-\sigma_y)}{(\phi_\infty - \phi_0) + \frac{1}{\sigma}\left[\frac{|\sigma-\sigma_y|}{K}\right]^{1/n}} \tag{11}$$

K and n are the consistency and flow behavior indexes respectively. $H(\sigma-\sigma_y)$ is the Heaviside step function which is equal to 1 when $\sigma > \sigma_y$, otherwise it is equal to zero. As a result, ϕ_{eq}^* is equal to zero when the stress is lower than the yield stress. Then, the fluidity (ϕ_v) is equal to the minimum possible value of fluidity (ϕ_0).

Looking back the boundary conditions shown in Fig. (3), it is possible to appreciate the necessity of imposing a coherent velocity profile at the capillary inlet. In fact, this velocity profile corresponds to a fully developed flow at equilibrium condition. Furthermore, this profile should be obtained from Eq. (11). If Eqs. (3), (11) & (5) are combined and considering that $\phi_\infty >> \phi_0$, Eq. (12) is obtained.

$$\dot{\gamma} = -\frac{dv_z}{dr} = \frac{\sigma H(\sigma-\sigma_y)}{\eta_\infty + \frac{\sigma}{[(\sigma-\sigma_y)/K]^{1/n}}} \tag{12}$$

η_∞ is just the reciprocal of ϕ_∞. For integrating Eq. (12) , it is necessary to consider the no-slip condition at the capillary wall (i.e., $v_z \to 0$ when $r \to R$). Where, R is the capillary radius. Then, it is possible to estimate the velocity in a particular location at the capillary inlet. In addition, we used a non-dimensional parameter ξ to get the velocity profile expressed by Eq. (13). This variable ξ is just a non-dimensional radius of the capillary (r/R).

$$v_z = \int_r^R \frac{\sigma H(\sigma-\sigma_y)}{\eta_\infty + \frac{\sigma}{[(\sigma-\sigma_y)/K]^{1/n}}} dr = \int_\xi^1 \frac{H(\sigma-\sigma_y)}{(\sigma_w\xi)^{-1}\eta_\infty + K^{1/n}[\sigma_w\xi - \sigma_y]^{-1/n}} d\xi \tag{13}$$

σ_w is the wall stress. If $\sigma \leq \sigma_y$, $\dot{\gamma} \to 0$ and v_z tends to be constant and equal to the maximum velocity at the domain (Estimated when $\sigma = \sigma_y$ on Eq. (13)). The solution of Eq. (13) could be numerical or analytical, depending on the rheological parameters introduced. For instance, σ_y is considered equal to zero to obtain an analytical velocity profile. σ_y was just discarded on the thixotropic flow through the capillary for numerical convenience. In the coating example presented in this paper, σ_y corresponds to the value of a laponite suspension obtained by de Souza Mendes *et al.* (2018).

Since $\sigma_y = 0$, the function $H(\sigma-\sigma_y)$ is equal to 1. Then, Eq. (13) is possible to solve by applying the Newton's binomial theorem. As a result, there are two possible solutions which can be found as follows:

$$v_z = \frac{R}{1/n+1}\left(\frac{\sigma_w}{K}\right)^{1/n}\left[{}_2F_1(a,b;c;d|_{\xi=1}) - (\xi)^{1/n+1}\,{}_2F_1(a,b;c;d|_{\xi})\right] \tag{14}$$

$$v_z = \frac{R\sigma_w}{2\eta_\infty}\left[{}_2F_1(a^*,b^*;c^*;d^*|_{\xi=1}) - (\xi)^2\,{}_2F_1(a^*,b^*;c^*;d^*|_{\xi})\right] \tag{15}$$

${}_2F_1(a,b;c;d|_\xi)$ and ${}_2F_1(a^*,b^*;c^*;d^*|_\xi)$ are Gaussian hypergeometric functions, which can be found in Eq. (16) and Eq. (17) respectively. $(a)_i$, $(b)_i$, and $(c)_i$ or $(a^*)_i$, $(b^*)_i$, and $(c^*)_i$ are Pochhammer symbols, which are rising factorial numbers in the way: $(a)_i = a(a+1)(a+2)(a+3)...(a+i-1)$. Hypergeometric functions converge if $|d|$ or $|d^*|$ are lower than 1 (Becken and Schmelcher, 2000). Consequently, Eq. (14) is valid if $|d| < 1$, otherwise Eq. (15) would be employed. Eq. (14) resembles the velocity profile obtained from the Herschel-Bulkley (HB) model. Actually, the latter was used as initial guess in the simulations.

$${}_2F_1(a,b;c;d|_\xi) = \sum_{i=0}^{\infty}\frac{(a)_i(b)_i}{(c)_i}\frac{d^i}{i!} \text{ where, } a=1,\ b=\frac{n+1}{1-n},\ c=-\frac{2}{n-1},\ d=-\frac{\eta_\infty\left(\frac{K}{\sigma_w\xi}\right)^{\frac{n-1}{n}}}{K} \tag{16}$$

$${}_2F_1(a^*,b^*;c^*;d^*|_\xi) = \sum_{i=0}^{\infty}\frac{(a^*)_i(b^*)_i}{(c^*)_i}\frac{(d^*)^i}{i!} \text{ where, } a^*=1,\ b^*=\frac{2n}{n-1},\ c^*=\frac{3n-1}{n-1},\ d^*=-\frac{K}{\eta_\infty\left(\frac{K}{\sigma_w\xi}\right)^{\frac{n-1}{n}}} \tag{17}$$

As mentioned before, it is necessary to solve the differential equation Eq. (7) in the case of a thixotropic liquid flow. For this particular equation, the Galerkin method is not good enough. So, the Petrov-Galerkin/Finite Element Method was employed in this case. In addition, it is necessary to have the function $f\left[\phi^*_{eq}(\sigma),\phi^*_v\right]$. Actually, de Souza Mendes *et al.* (2018) provide this function for a Laponite suspension Eq. (18). t_c is usually a fixed value and equal to 663 s (used in all simulations in the present work) while t_a is estimated by Eq. (19). The exponent (s) is estimated by Eq. (20). As boundary condition for Eq. (7), we assumed a fully developed flow at the capillary inlet. In addition, it is assumed that thixotropic liquid achieved an equilibrium condition before entered into the domain. This condition is related to a given wall liquid's stress (σ_w). As a result, it is possible to estimate the fluidity profile at the capillary inlet by using Eq. (11).

$$f\left[\phi^*_{eq},\phi^*_v\right] = \begin{cases} \frac{s}{t_a\phi^*_{eq}(\sigma)}\left(\phi^*_{eq}-\phi^*_v\right)^{\frac{s+1}{s}}{\phi^*_v}^{\frac{s-1}{s}} & 0<\phi^*_v\le\phi^*_{eq} \\ -\frac{(\phi^*_v-\phi^*_{eq})}{t_c} & \phi^*_{eq}<\phi^*_v\le 1 \end{cases} \tag{18}$$

$$t_a = 59.2\frac{(1-\phi^*_{eq})^{1.1}}{{\phi^*_{eq}}^{0.4}} \tag{19}$$

$$s = \frac{8.0}{exp(\phi^*_{eq}/0.09)-1} + 1.2 \tag{20}$$

2.2 thixotropic flows into a slot coating device near the downstream meniscus

The main features of the slot coating section, that we studied in the simulations, can be found in Fig. 4 . *Q* is the imposed volumetric flow rate (per unit width). Consequently, the film thickness (*h*) just depends on the values of flow rate (*Q*) and the moving plate's velocity (*U*). The coating gap (H_0) value is equal to 0.1 mm.

The respective boundary conditions are also included in Fig. 4. The typical no-slip condition is considered on the solid walls. In the case of the free surface, it is necessary to take into consideration other issues. For example, there is no liquid flux across the free surface (where $\mathbf{n}$ and $\mathbf{t}$ are local unit normal and tangent vectors respectively). In addition, the liquid traction must balance the pressure in the ambient gas and the capillary pressure because of the meniscus curvature (Rebouças *et al.*, 2018). As a result, the stress jump across the surface can be written as $\mathbf{n}\cdot\boldsymbol{\sigma} = (-P_g+\gamma\kappa)\mathbf{n}$; where P_g, γ, and κ are the gas pressure, the liquid's superficial tension, and the free surface curvature respectively (Rebouças *et al.*, 2018).

To define the velocity profile at the slot inlet, it is necessary to establish the kind of flow that we have between the plates. As a first approximation, the flow can be defined as *Couette flow*, where the pressure gradients are neglected.

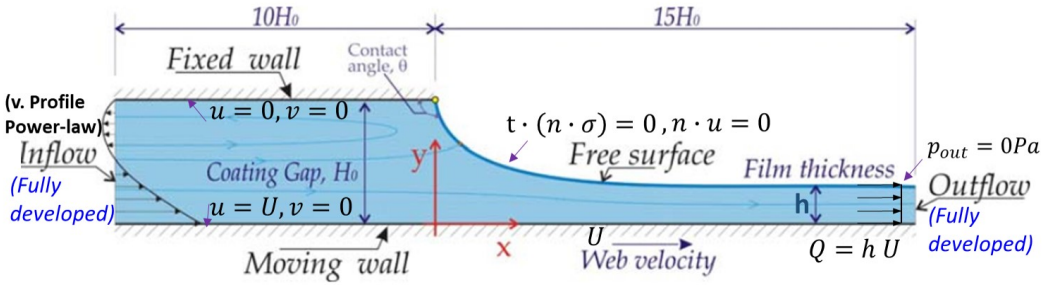

Figure 4. Sketch of the downstream section of the slot coating device

However, this approximation is just valid if the (h/H_0) ratio is equal to 0.5 even for Newtonian fluids. Schlichting (1955), as cited by Flumerfelt *et al.* (1969), superposed the solution of two problems to get the so-called *generalized Couette flow* solution. One of the problems consists in flow between two parallel solid walls, one of them is moving, and no pressure gradient. The second problem is flow between two fixed parallel walls as a result of a pressure gradient. The superposition of these solutions is widely employed for Newtonian fluids, and it is even able to model backflow in a very good manner. Nevertheless, the quadratic velocity profile obtained for Newtonian fluids gives poor predictions in the case of non-Newtonian fluids. Then, the superposition of the problems, just explained before, is not possible for the latter kind of fluids. Consequently, Flumerfelt *et al.* (1969) propose an alternative approach, using the Power-law model, to get a more appropriate velocity profile .

Considering the pressure gradient at the slot inlet and the Power-law model, it is possible to express the stress at the inlet as Eq. (21). ξ is the non-dimensional ratio y/H_0 while β is a non-dimensional parameter that depends on the value of Q.

$$\sigma_{yx} = -K\left|\frac{dv_x}{dy}\right|^{n-1}\left(\frac{dv_x}{dy}\right) = -\left(\frac{P_0 - P_L}{L}\right)H_0(\beta - \xi) \tag{21}$$

Introducing the non-dimensional velocity (θ), which is equal to v_x/U, it is possible to rewrite Eq. (21) as follows:

$$\left|\frac{d\theta}{d\xi}\right|^{n-1}\left(\frac{d\theta}{d\xi}\right) = \Lambda(\beta - \xi) \text{ where, } \Lambda = \left(\frac{H_0}{U}\right)^n\left(\frac{P_0 - P_L}{L}\right)\frac{H_0}{K} \tag{22}$$

Depending on the value of β, there are two possibilities. Firstly, if $\beta > 1$ (Case I), there is no recirculation or backflow (i.e., $\theta \geq 0$ in the whole domain). Otherwise, it is expected to register backflow and part of the coating liquid will be recirculated (Case II). Figure 5 shows both cases in more detail.

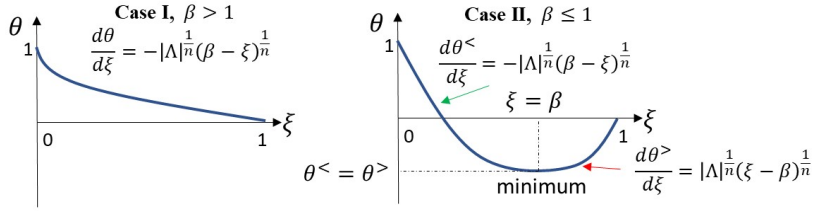

Figure 5. Sketch (not-to-scale) of the velocity profiles for: a) Case I ($\beta > 1$)), b) Case II ($\beta \leq 1$).

In our case, we did not study thixotropic coating backflow. Therefore, It was just considered the case I ($\beta > 1$) from Fig. 5 . Then the velocity profile at the inlet, for $\beta > 1$, is obtained by integration and evaluation of the non-dimensional boundary conditions. Actually, it can be found as Eq. (23). A non-dimensional volume (Ω) equal to $Q/(UH_0)$ is also presented. In fact, β depends on the latter parameter as shown in Eq. (24). In a straightforward manner, it is possible to demonstrate that $\Omega = h/H_0$. It is also relatively easy to obtain the expression Eq. (25) to determine the critical h/H_0 ratio, which is called Ω_{crit}. The latter parameter predicts when backflow in expected. In other words, if $\Omega > \Omega_{crit}$, liquid recirculation would not be expected for a generalized Newtonian liquid.

$$\theta = 1 - \frac{|\Lambda|^{1/n}}{1/n+1}[\beta^{1/n+1} - (\beta - \xi)^{1/n+1}] \text{ where, } \frac{|\Lambda|^{1/n}}{1/n+1} = \frac{1}{\beta^{1/n+1} - (\beta - 1)^{1/n+1}} \tag{23}$$

$$\Omega = \frac{h}{H_0} = \int_0^1 \theta d\xi = 1 + \frac{1}{(\beta-1)^{1/n+1} - \beta^{1/n+1}} \left[\frac{(\beta-1)^{1/n+2} - \beta^{1/n+2}}{1/n+2} + \beta^{1/n+1} \right] \tag{24}$$

$$\Omega_{crit} = 1 - \frac{1/n+1}{1/n+2} \tag{25}$$

After solving the velocity profile issue, it is possible to solve the mass and momentum conservation equations (Eqs. (9) and (10) respectively). In the case of the GNM liquid, it is only needed Eq. (11) to estimate the fluidity (i.e., reciprocal of fluidity). On the other hand, in the case of a thixotropic flow; it is also necessary to solve Eq. (7). The boundary condition at the slot inlet, for the last equation, is obtained from the fluidities got from Eq. (11). However, it is important to notice that the fluidities are estimated by evaluating $|\sigma_{yx}|$ on Eq. (11). It is relatively easy to obtain an expression of $|\sigma_{yx}|$, which includes σ_y as well. Actually, Eq. (26) can be employed to estimate the fluidities at the inlet (considering fully developed flow and equilibrium condition).

$$|\sigma_{yx}| = \left(\frac{P_0 - P_L}{L} \right) H_0(\beta - \xi) + \sigma_y \tag{26}$$

3. RESULTS AND DISCUSSION

All results were obtained by using the following rheological parameters: $K = 1$ Pa.s^n, $n = 0.32$, and $\phi_\infty = 64.1$ (Pa.s)$^{-1}$, which corresponds to a real Laponite suspension obtained by de Souza Mendes *et al.* (2018). In the same way, the avalanche time (t_a) is estimated by using Eq. (19) while the construction time (t_c) is fixed in 663 s. The value of ϕ_0 was fixed in 10^{-3} (Pa.s)$^{-1}$ for numerical convenience. Regarding the yield stress (σ_y), a value of 6 Pa was used in the simulations of slot coating flows while it was neglected in the cases of flows throught the capillary due to numerical reasons. Two graphs of the fluidity (ϕ_v) vs σ, for the Laponite suspension just mentioned before, are shown in Fig. 6 . One of the graph is for $\sigma_y = 6\ Pa$ while the graph at the right is for $\sigma_y = 0\ Pa$.

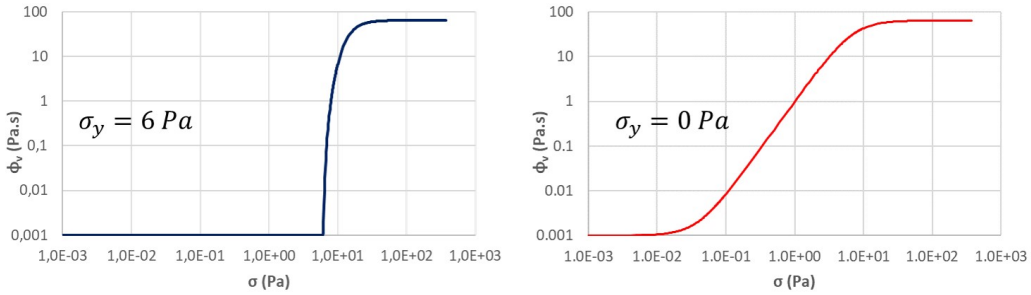

Figure 6. Fluidity vs stress for laponite suspensions with $\sigma_y = 6\ Pa$ and $\sigma_y = 0\ Pa$

3.1 Results of thixotropic flows through a constricted capillary

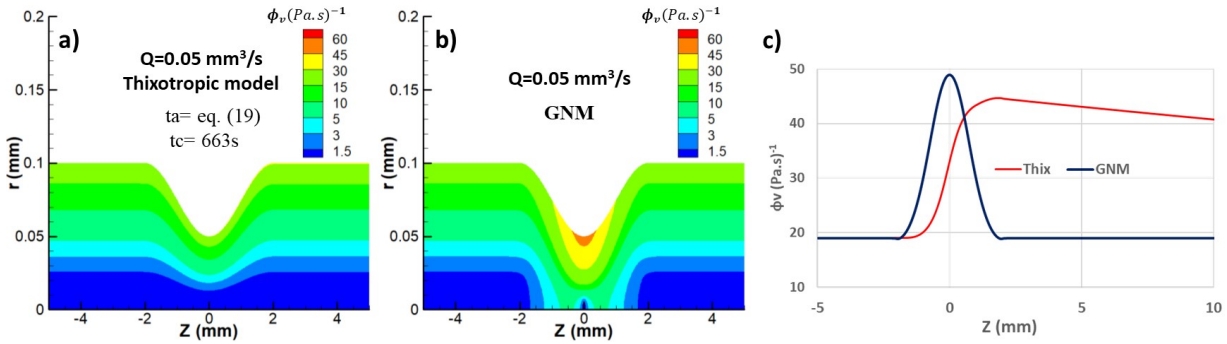

Figure 7. a) Fluidity field for a thixotropic liquid, b) Fluidity field for a GNM liquid, c) Comparison between fluidity values of thixotropic (Thix) and GNM liquids at the capillary wall

Figure 7 shows a comparison between two fluidity fields obtained from thixotropic and GNM simulations (For a Q = 0.05 mm^3/s). In this case, the effects in the constriction are observed in more detail taking a zoom of the domain (Z=-5 mm to Z=+5 mm). Then, it is possible to appreciate that the constriction provokes a perturbation in the equilibrium condition, and the response of the liquid is different according to the model (i.e., thixotropic and GNM). For instance, there is much more destruction of the microstructure close to the capillary wall constriction according to the GN model. As a result, the fluidity values are much higher near this area than those obtained from the thixotropic model. This is more evident looking at the fluidity profile measured at the wall shown in Fig. 7c. Then, it is expected much lower friction and pressure drop due to much lower viscosity values (i.e., viscosity is the reciprocal of fluidity) by using the GNM flow, as reflected in Fig. 8.

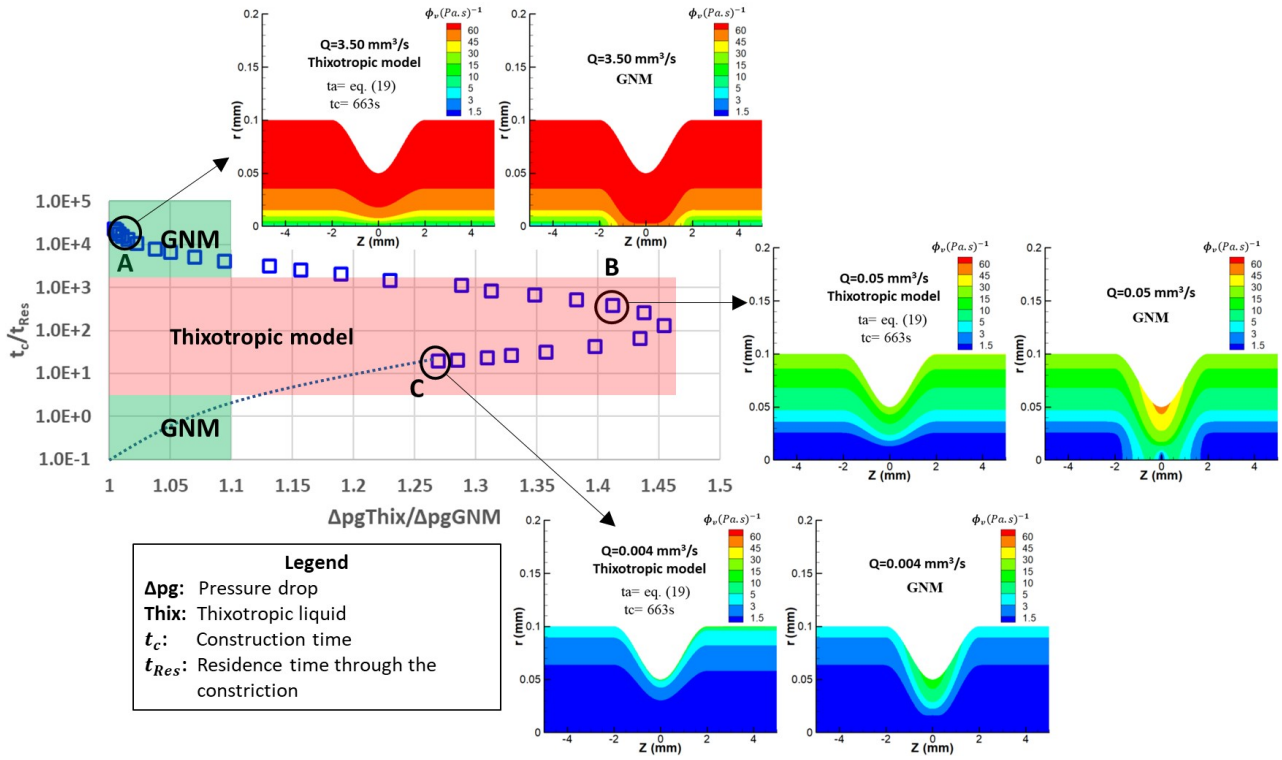

Figure 8. t_c/t_{Res} vs $\Delta p_{Thix}/\Delta p_{GNM}$ for a idealized suspension of Laponite with $\sigma_y = 0\ Pa$, including thixotropic and GNM fluidity fields for Q = 3.5, 0.05, and 0.004 mm^3/s

Figure 8 shows a variation of the $\Delta p_{Thix}/\Delta p_{GNM}$ ratio with the t_c/t_{Res} ratio. In addition, it is good to remind that t_{Res} is inversely proportional to Q. In other words, as Q increases, t_{Res} decreases. The pressure drop for both thixotropic and GNM liquids is estimated just before and after the construction (i.e., z = -10 mm and z = +10 mm). Likewise, stable flow is ensured at the measuring points. Furthermore, the pressure drop at the constriction is emphasized at the same time.

The cases A, B and C from Fig. 8 correspond to Q = 3.50, 0.05, and 0.004 mm^3/s respectively. Firstly, the case A represents large values of t_c/t_{Res}. As a result, t_{Res} is too short for the thixotropic flow to feel the equilibrium perturbation provoked by the constriction. On the other hand, the GNM simulation predicted more destruction of the liquid's microstructure close to the symmetry axis. Nevertheless, the microstructure is highly destroyed (as reflected the values in fluidity close to the maximum value of $64.1(Pa.s)^{-1}$) near the capillary wall constriction in both thixotropic and GNM flows. Hence, the fiction is similar according to the thixotropic and GNM simulations for the A's t_c/t_{Res} ratio. As a result, the ratio $\Delta p_{Thix}/\Delta p_{GNM}$ is near to 1. Then, it is possible to employ the generalized Newtonian model (GNM) in thixotropic modeling for large Q (e.g., t_c/t_{Res} values larger than 10^4).

On the other hand, as t_c/t_{Res} decreases, the ratio $\Delta p_{Thix}/\Delta p_{GNM}$ increases. Therefore, the thixotropic flows tend to behave much differently near the constriction's wall as Q diminishes. For example in the case B, where the difference in pressure drop is close to 45%. It implies that the characteristic thixotropic times have to be taken into account in this range of t_c/t_{Res} (e.g., 1 to 10^4).

However, the ratio $\Delta p_{Thix}/\Delta p_{GNM}$ achieves a maximum value of about 1.45. Then, the pressure drops ratio decreases as shown in Fig. 8 from the point B to C. Actually, in the latter case there are more similarities in the fluidity values between the thixotropic and GNM simulations than in the case B. In addition, it is possible to appreciate a noticeable delayed phenomenon in the microstructure destruction for the thixotropic flow. If the ratio t_c/t_{Res} keeps decreasing, t_{Res} of the liquid will eventually be large enough to allow it to respond the equilibrium perturbation at the constriction. Then, the thixotropic liquid is expected to behave similarly to the GNM one for large t_{Res}.

3.2 Results of thixotropic flows into a slot coating device near the downstream meniscus

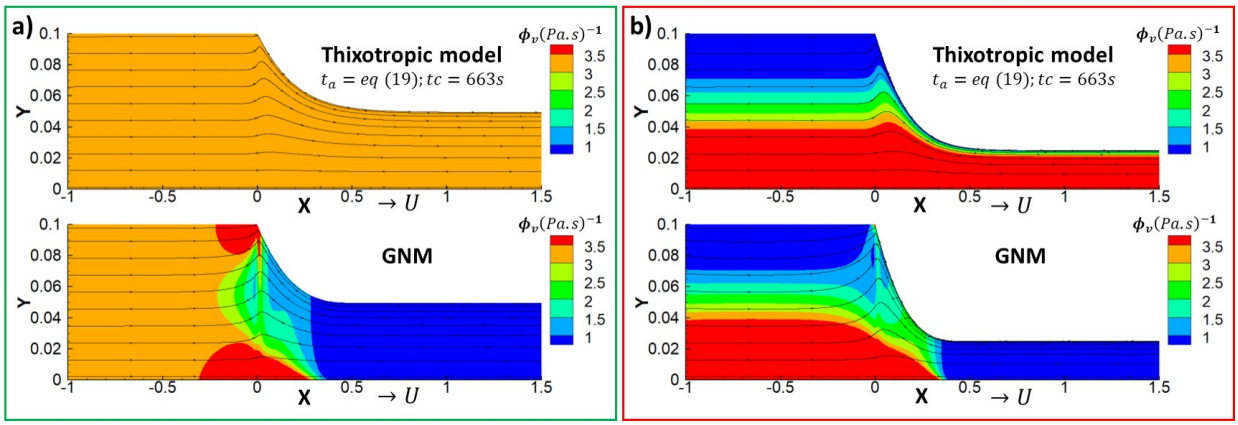

Figure 9. Fluidity fields for Thixotropic and GNM flows near the downstream meniscus for a) h/H_0=0.495, b) h/H_0=0.25

Figure 9 shows a comparison between thixotropic and GNM simulations for two h/H_0 ratios (0.495 and 0.25 respectively). The moving plate's velocity (U) is 3 mm/s. At the left, we have an approximation to a Couette flow. So, the pressure drop at the slot is very small. Then, we have a constant or almost constant stress at the inlet. So, the fluidity is almost constant at the inlet in both cases (GNM and thixotropic flow). On the other hand, the fluidity profiles for h/H_0 equal to 0.25 show that the Couette approximation is not valid for this ratio. Actually, the variety of values in fluidity reflects that the stress is not almost constant anymore. For both h/H_0 ratios, the thixotropic liquid tend to keep the inlet fluidity values along the domain. Nevertheless, the GNM liquid develops other response as goes into slot and under the free surface. Since the thixotropic liquid has much larger characteristic times than its residence time (t_c/t_{Res} is about 796 on the moving plate from x = -1 to x = +1.5 mm), so it's not possible to accommodate itself to the new equilibrium condition. Besides the differences between the thixotropic and GNM fluidity fields, the fluidity values at the slot's inlet are the same. Then, it is possible to say that the velocity profile obtained from the Power-law model sucessfully describes the studied slot coating flows.

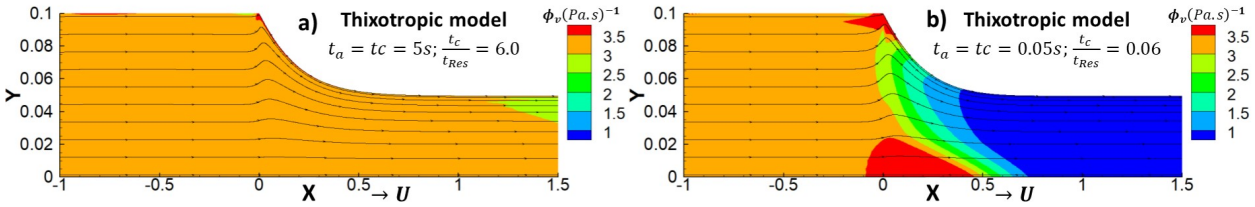

Figure 10. Fluidity fields thixotropic flows with (h/H_0=0.495) near the downstream meniscus for reduced characteristic times: a) t_a=t_c= 5s, t_c/t_{Res}= 6.0 ; b) t_a=t_c= 0.05s, t_c/t_{Res}= 0.06

To obtain the fluidity fields shown in Fig. 10, both t_a and t_c were fixed. Then, both characteristic times were reduced. Initially, the fluidity values were very similar to those registered for the thixotropic simulation (with h/H_0=0.495) shown in Fig. 9. However, some differences appear as t_a and t_c decrease. For instance, the fluidity field Fig. 10a shows some differences compared to the thixotropic fluidity field Fig. 9a. Furthermore, as t_c/t_{Res} ratio keeps decreasing the fluid tends to behave similarly to the GNM liquid. For example, the fluidity field Fig. 10b resembles the GNM liquid field from Fig. 9a.

4. CONCLUSIONS

A novel rheological model, based on fluidity, was used. The system of equations consisting of continuity, momentum, and fluidity equations was solved by using the Galerkin and Petrov-Galerkin / Finite Element Method. As a result, fluidity fields, and pressure drop values were obtained for a Laponite suspension flow into a capillary and slot coating device.

Most flow analyses of particle suspensions oversimplify the rheological modeling. For instance, the use of simple viscosity equations like generalized Newtonian models. Furthermore, neglecting time dependency, by only considering viscosity as a function of the local shear rate, may completely misrepresent the flow phenomena. Consequently, time dependency should be considered in thixotropic flows to model them accurately. Although if the residence time of the liquid tends to be zero or if the t_c/t_{Res} ratio is much shorter than 1, solutions from a generalized Newtonian model are valid as well.

5. ACKNOWLEDGEMENTS

The authors aknowledge CAPES and CNPQ for financial support.

6. REFERENCES

Barnes, H.A., 1997. "Thixotropy—a review". *Journal of Non-Newtonian Fluid Mechanics*, Vol. 70, No. 1, pp. 1–33. ISSN 0377-0257.

Becken, W. and Schmelcher, P., 2000. "The analytic continuation of the gaussian hypergeometric function ${}_2F_1$(a,b;c;z) for arbitrary parameters". *Journal of Computational and Applied Mathematics*, Vol. 126, No. 1, pp. 449–478. ISSN 0377-0427.

Carvalho, M.S. and Kheshgi, H.S., 2000. "Low-flow limit in slot coating: Theory and experiments". *AIChE Journal*, Vol. 46, No. 10, pp. 1907–1917.

de Souza Mendes, P.R., 2009. "Modeling the thixotropic behavior of structured fluids". *Journal of Non-Newtonian Fluid Mechanics*, Vol. 164, No. 1, pp. 66–75. ISSN 0377-0257.

de Souza Mendes, P.R., Abedi, B. and Thompson, R.L., 2018. "Constructing a thixotropy model from rheological experiments". *Journal of Non-Newtonian Fluid Mechanics*, Vol. 261, pp. 1–8. ISSN 0377-0257.

de Souza Mendes, P.R. and Thompson, R.L., 2012. "A critical overview of elasto-viscoplastic thixotropic modeling". *Journal of Non-Newtonian Fluid Mechanics*, Vol. 187-188, pp. 8–15. ISSN 0377-0257.

de Souza Mendes, P.R. and Thompson, R.L., 2013. "A unified approach to model elasto-viscoplastic thixotropic yield-stress materials and apparent yield-stress fluids". *Rheologica Acta*, Vol. 52, pp. 673–694. ISSN 1435-1528.

Eberhard, U., Seybold, H.J., Floriancic, M., Bertsch, P., Jiménez-Martínez, J., Andrade, J.S. and Holzner, M., 2019. "Determination of the effective viscosity of non-Newtonian fluids flowing through porous media". *Frontiers in Physics*, Vol. 7. ISSN 2296-424X.

Flumerfelt, R.W., Pierick, M.W., Cooper, S.L. and Bird, R.B., 1969. "Generalized plane couette flow of a non-Newtonian fluid". *Industrial & Engineering Chemistry Fundamentals*, Vol. 8, No. 2, pp. 354–357.

Fredrickson, A.G., 1970. "A model for the thixotropy of suspensions". *AIChE Journal*, Vol. 16, No. 3, pp. 436–441.

Glass, J.E. and Prud'homme, R.K., 1997. "Coating rheology: Component influence on the rheological response and performance of water-borne coatings in roll applications". In S.F. Kistler and P.M. Schweizer, eds., *Liquid Film Coating: Scientific principles and their technological implications*, Springer Netherlands, Dordrecht, chapter 5, pp. 137–183. ISBN 978-94-011-5342-3.

Kisler, S.F. and Schweizer, P.M., 1997. "Coating science and technology: An overview". In S.F. Kistler and P.M. Schweizer, eds., *Liquid Film Coating: Scientific principles and their technological implications*, Springer Netherlands, Dordrecht, chapter 1, pp. 137–183. ISBN 978-94-011-5342-3.

Mewis, J. and Wagner, N.J., 2009. "Thixotropy". *Advances in Colloid and Interface Science*, Vol. 147-148, pp. 214–227. ISSN 0001-8686. Colloids, polymers and surfactants.Special Issue in honour of Brian Vincent.

Moisés, G., Alencar, L., Naccache, M. and Frigaard, I., 2018. "The influence of thixotropy in start-up flow of yield stress fluids in a pipe". *Journal of Petroleum Science and Engineering*, Vol. 171, pp. 794–807. ISSN 0920-4105.

Pritchard, D., Wilson, S.K. and McArdle, C.R., 2016. "Flow of a thixotropic or antithixotropic fluid in a slowly varying channel: The weakly advective regime". *Journal of Non-Newtonian Fluid Mechanics*, Vol. 238, pp. 140–157. ISSN 0377-0257. Viscoplastic Fluids From Theory to Application 2015 (VPF6).

Rebouças, R., Siqueira, I. and Carvalho, M., 2018. "Slot coating flow of particle suspensions: Particle migration in shear sensitive liquids". *Journal of Non-Newtonian Fluid Mechanics*, Vol. 258, pp. 22–31. ISSN 0377-0257.

Siqueira, I.R., Pasquali, M. and de Souza Mendes, P.R., 2020. "Couette flows of a thixotropic yield-stress material: Performance of a novel fluidity-based constitutive model". *Journal of Rheology*, Vol. 64, No. 4, pp. 889–898.

Sochi, T., 2010. "Non-Newtonian flow in porous media". *Polymer*, Vol. 51, No. 22, pp. 5007–5023. ISSN 0032-3861.

7. RESPONSIBILITY NOTICE

The authors are solely responsible for the printed material included in this paper.